

Single cell versus large population analysis: cell variability in elemental intracellular concentration and distribution

Emil Malucelli¹ · Alessandra Procopio¹ · Michela Fratini^{2,3} · Alessandra Gianoncelli⁴ · Andrea Notargiacomo⁵ · Lucia Merolle⁶ · Azzurra Sargenti¹ · Sara Castiglioni⁷ · Concettina Cappadone¹ · Giovanna Farruggia^{1,8} · Marco Lombardo⁹ · Stefano Lagomarsino³ · Jeanette A. Maier⁷ · Stefano Iotti^{1,8}

Received: 1 June 2017 / Revised: 13 October 2017 / Accepted: 25 October 2017 / Published online: 17 November 2017
© Springer-Verlag GmbH Germany 2017

Abstract The quantification of elemental concentration in cells is usually performed by analytical assays on large populations missing peculiar but important rare cells. The present article aims at comparing the elemental quantification in single cells and cell population in three different cell types using a new approach for single cells elemental analysis performed at sub-micrometer scale combining X-ray fluorescence microscopy and atomic force microscopy. The attention is focused on the light element Mg, exploiting the opportunity to compare the single cell quantification to the cell population analysis carried out by a highly Mg-selective fluorescent chemosensor. The results show that the single cell analysis reveals the same Mg differences found in large population of the different cell strains studied. However, in one of the cell strains, single cell analysis reveals two cells with an exceptionally high intracellular Mg content compared with the other cells of the same strain. The single cell analysis allows mapping Mg and other light elements in whole cells at sub-

micrometer scale. A detailed intensity correlation analysis on the two cells with the highest Mg content reveals that Mg subcellular localization correlates with oxygen in a different fashion with respect the other sister cells of the same strain.

Keywords Light elements quantification · Magnesium · Synchrotron-based X-ray fluorescence microscopy · Fluorescent chemosensors · Single cells analysis

Introduction

Single cell analysis has become increasingly important for cellular biologists doing basic, translational, and clinical research. Cell populations are known to be heterogeneous and there are evidences showing that heterogeneity exists even within small cell populations [1, 2]. However, most of the current techniques collect bio-data averaged over a large pop-

Electronic supplementary material The online version of this article (<https://doi.org/10.1007/s00216-017-0725-8>) contains supplementary material, which is available to authorized users.

✉ Emil Malucelli
emil.malucelli@unibo.it

¹ Department of Pharmacy and Biotechnology, University of Bologna, 40127 Bologna, Italy

² Museo Storico della Fisica e Centro Studi e Ricerche Enrico Fermi, Piazza del Viminale, 1, 00184 Roma, Italy

³ CNR-Nanotec, c/o Department of Physics University Sapienza, Rome, Italy

⁴ Elettra - Sincrotrone Trieste, Basovizza, 34149 Trieste, Italy

⁵ Consiglio Nazionale delle Ricerche, Institute for Photonics and Nanotechnology, 00156 Rome, Italy

⁶ Arcispedale S. Maria Nuova-IRCCS, Viale Risorgimento 80, 42123 Reggio Emilia, Italy

⁷ Department of Biomedical and Clinical Sciences “L. Sacco”, University of Milan, 20157 Milan, Italy

⁸ National Institute of Biostructures and Biosystems, 00136 Rome, Italy

⁹ Department of Chemistry “G. Ciamician”, University of Bologna, 40126 Bologna, Italy

ulation of cells rather than considering their distribution, missing rare (but important) cells that are only present in small quantity. Cell populations often exhibit phenotypic heterogeneity that could lead to a misleading interpretation of the results since individual cells may also differ with respect to the population observed [3–5] as well-documented in bacteria and in eukaryotic cells [6]. In the literature there are studies showing that variability in protein expression can be considerable from cell to cell, affecting signaling networks and, therefore, the related biological outcomes [7, 8]. In one of these studies it has been hypothesized that an average of 50% protein expression in a cell population can represent either a 100% response in half of the cells or a 50% response in all [8]. Consequently, single-cell analysis is a fast growing field with a high impact in the research community owing to its numerous applications including cancer research, diagnostic, and drug discovery [8]. On the other hand, multiple individual cells are required to obtain statistically meaningful data; therefore the interpretation of the results is critical in terms of the applied statistics. The analysis of cell populations can be challenging when the number of cells is small as reported by Mark et al. [9] in the isolation of RNA from K-562 leukemia cells. The strategy to overcome this issue is to characterize each single cell of a population but, obviously, this is not always possible. Nowadays, single cell analysis is a potent tool mainly used in ‘omics’ studies including metabolomics, transcriptomics, proteomics, and genomics [10]. Nevertheless, single cells analysis applied to the intracellular elemental quantification is still taking the first steps and it is far away from being validated with other conventional techniques used in populations of cells. Within this framework, in the present study, we aimed at comparing the intracellular elemental quantification in single cells and cell population exploiting a new analytical approach recently developed for single cells element analysis. We showed the possibility to assess the intracellular concentration of the so-called light elements (C, N, O) and light metals (Na and Mg) using a multimodal approach, combining synchrotron X-Ray fluorescence microscopy (XRFM) with atomic force microscopy (AFM) [11, 12]. XRFM is a promising technique based on synchrotron high brilliance light source, highly sensitive for mapping elemental distribution in single cells at nanoscale resolution [13, 14]. It has been used for mapping both light elements [11, 12] and transition metals (Cr, Mn, Fe, Co, Ni, Cu, Zn, Cd, etc.) [15–17].

In this study, we focused on Mg exploiting the opportunity to compare the single cell quantification performed by XRFM-AFM to the cell population analysis carried out by fluorescence assay. We used the fluorescent dye DCHQ5 able to quantify the total intracellular Mg concentration in cell populations [18]. Comparing the analytical performance of DCHQ5 with flame atomic absorption spectroscopy (F-AAS), we previously showed that DCHQ5 allowed scaling down by almost two orders of magnitude the number of cells

to be analyzed, obtaining comparable results to F-AAS [19]. Beside the analytical advantage offered by DCHQ5, this also means that the value of total intracellular Mg assessed in millions of cells equals that measured in tens of thousands. Now the question is: “What happens if we drastically decrease the cell population by another three orders of magnitude?”. Moreover, the choice of Mg is not merely analytical. The metabolism of this element still retains many aspects to disclose, although the magnesium homeostasis cannot be considered anymore a mystery as it was till the end of the last century [20]. There are still many regulatory aspects involving Mg that keep their secrets. In recent years, thanks to chemical imaging techniques able to characterize the chemical composition of cells, several progresses have been made in the comprehension of the fundamental biological process at the cellular and sub-cellular level [21–24]. Knowledge of the intracellular concentration and distribution of the chemical elements in cells may reveal their function in a variety of cellular processes. The biological function of a chemical element in cells does not only require the determination of its intracellular quantity but also the spatial distribution of its concentration [25].

In this study, the comparison of the Mg assessment in single cell and cell population was performed in three different human cell lines: HUVEC, SaOS2, and LoVo. Each strain was divided in two populations: one taken as control and the others treated specifically to generate potential variation of intracellular Mg content and distribution.

Experimental

Cell preparation

We employed three different cell types, i.e. primary HUVEC isolated from the umbilical vein (American Type Culture Collection), human osteoblast-like SaOS2 (American Type Culture Collection HTB-85), and colon carcinoma LoVo cells (kindly donated by Dr. P. Perego, Istituto Nazionale Tumori, Milano).

We studied HUVEC and HUVEC genetically engineered to silence TRPM7 (HUVEC^{-TRPM7}), which is essential to maintain intracellular Mg homeostasis [26]. To obtain TRPM7 silencing, HUVECs were stably transfected with pTRIPZ inducible siRNA vector (Dharmacon, GE Healthcare) containing a specific siRNA sequence for TRPM7. The vector contains the puromycin resistance and is engineered to be Tet-On and to produce tightly regulated induction of siRNA expression in the presence of doxycycline. The pTRIPZ vector was transfected using Arrest-In transfection reagent (Open Biosystems). Transfected clones were isolated and maintained in a culture medium containing 0.3 µg/mL puromycin. To induce shRNA TRPM7 expression, transfected cells were cultured in a medium containing doxycycline at a concentration

of 0.5 $\mu\text{g}/\text{mL}$ for 48 h. In addition to driving expression of the shRNA, the tetracycline-inducible promoter also drives the expression of a TurboRFP reporter for visual tracking of shRNA expression. Transfected cells, which express the siRNA are visualized in red at microscope (see Electronic Supplementary Material (ESM) Fig. S4). Five HUVEC and five HUVEC^{-TRPM7} cells were used for single cell analysis whereas DCHQ5 fluorimetric assay was performed in samples of 100,000 cells.

SaOS2 cells were cultured in a Mg-free medium containing 0.5% FBS to synchronize cells in G0/G1 phase and reduce intracellular Mg content (ESM Fig. S1). After 24 h of starvation, control cells (SaOS2^{+Mg}) were cultured for an additional 24 h in the presence of 1 mM Mg, while Mg-deficient cells (SaOS2^{-Mg}) were maintained for the following 24 h in Mg free medium. Four SaOS2^{+Mg} and four SaOS2^{-Mg} cells were used for single cell analysis while DCHQ5 fluorimetric assay was performed in samples of 100,000 cells.

LoVo sensitive (LoVo-S) and LoVo resistant (LoVo-R) to doxorubicin were cultured in RPMI with 10% FBS for 24 h at 37 °C and 5% CO₂. LoVo-R displayed a higher Mg content [11, 27] compared with the sensitive counterpart (LoVo-S). Fourteen LoVo-S and thirteen LoVo-R cells were used for single cell analysis, whereas DCHQ5 fluorimetric assay was performed in samples of 150,000 cells.

For single cell analysis, cells were plated at a concentration of 1×10^4 cell/cm² on 1×1 mm², 200-nm-thick silicon nitride (Si₃N₄) membrane windows, mounted on a 5×5 mm² Si frame (Silson) previously sterilized in ethanol.

In particular, the cells were seeded on a plate containing the silicon nitride windows. We carefully checked by optical microscopy that cell adhesion occurred regularly on both plate and silicon nitride surfaces. After cell adhesion, the sample was washed twice to clean up all the debris and nonadherent cells. Prior to seeding the cells, a cell cycle analysis was performed on a sister batch by flow cytometry to check the status of the cells.

Two dehydration methods were then followed. In the first case, at 50% – 80% confluency, cells were briefly rinsed in 150 mM KCl and then fixed in ice-cold methanol/acetone 1:1 and air-dried. This method has been used in five LoVo-S and four LoVo-R cells. In the second case, after rinsing with 100 mM ammonium acetate, cells were cryo-fixed by plunge freezing in liquid ethane bath cooled with liquid nitrogen [21] and then dehydrated in vacuum at low temperature overnight.

Quantification of total Mg by DCHQ5 chemosensor

Total Mg content was assessed on sonicated cells by using the fluorescent chemosensor DCHQ5 [18, 19]. Briefly, DCHQ5 was dissolved to a final concentration of 15 μM in a mixture that contains 10% of phosphate buffer saline without Ca and

Mg (PBS) in a solution 1:1 of MeOH:MOPS 2 mM (pH 7.4). To perform standard curve, different amounts of MgSO₄ were added and the fluorescence intensities were acquired at 510 nm. Mg concentrations of the samples were obtained by the interpolation of their fluorescence with the standard curve and were referred to the actual cell volume. For the assessment of the intracellular volume, cells were trypsinized and resuspended in PBS. Cell volume was calculated assessing the diameter cell profile by using a Z1 Beckman Coulter counter (Beckman Coulter). The cell volume is given in terms of equivalent spherical diameter (ESM Fig. S5). The analysis was carried out in triplicate.

Atomic force microscopy measurements

Cell thickness maps were collected using a Digital Instruments D3100 atomic force microscopy (AFM) equipped with a Nanoscope IIIa controller. Measurements were carried out in air in Tapping Mode at a resonance frequency of about 260 kHz by use of monolithic silicon tips with an apex curvature radius in the 5–10 nm range and a typical force constant of ~ 40 N·m⁻¹. The typical square scan size used was on the order of $50 \mu\text{m} \times 50 \mu\text{m}$, and the matrix resolution in pixels was 512×512 . For further detail on the AFM measurements see [11]. The cell boundaries were automatically delineated from the AFM thickness maps exploiting the intrinsically lower noise of AFM technique with respect to X-ray based imaging, which allows for a more precise definition of the cell shape. The masks of the cells obtained by the AFM segmentation have been used to mask out all the areas outside the cell (black pixel in the images). Moreover, the inverse of this mask has been utilized to calculate the background of all the maps.

X-ray fluorescence microscopy and scanning transmission microscopy measurements

X-ray fluorescence microscopy and scanning transmission X-Ray microscopy (STXM) measurements were carried out at the beamline TwiniMic [28] at Elettra Synchrotron (Trieste, Italy). A Fresnel zone plate focused the incoming beam (1475 eV), monochromatized by a plane grating monochromator, to a circular spot of about 600 nm in diameter. Five STXM images were acquired on whole cells with 25 ms dwell time per step, with a step size of 500 nm. In sequence, XRFM were carried out with a range of 6–8 s dwell time per pixel depending on the cell size. The total acquisition time for each XRFM scan was in the range of 7–9 h (field of view of at least $20 \times 20 \mu\text{m}^2$; spatial resolution 500 nm).

Elemental quantification

The elemental quantification was based on the method proposed by Malucelli et al. [11]. Briefly, the mass fraction W has been calculated merging the information coming from XRFM, STXM and AFM using the fundamental parameter equation [29]:

$$W(i) = \frac{R}{[\rho V][Y]F_p} \quad (1)$$

where V is the volume measured by AFM; ρ is the density calculated by the Beer-Lambert law (using cell thickness data obtained by AFM analysis), and considering a given cell composition taken from literature [30]. R is the contribution to the total counts for that specific fluorescence line derived by the analysis of X-ray fluorescence spectra using PyMCA software [31]. Y is a set of constants, some linked to the element measured such as the fluorescence yield, the transition probability, and the photon electron cross-section, and some linked to the characteristics of the beamline such as the detector efficiency and solid angle seen by the detector. The detector efficiency has been evaluated examining two standards: one comprised of a Mg film 200 nm thick covered by a Au film of 50 nm; and the other comprised of a bare 200 nm thick Si_3N_4 window, equal to those used as substrate for our samples. Finally, F_p is the correction factor for the self-absorption of both incident beam and fluorescence radiation, calculated using an ad hoc home-made algorithm [32].

The elemental molar concentration was calculated using the following equation:

$$M(i) = \frac{W(i) \times \rho}{A_i} \quad (2)$$

where A_i is the atomic weight of the i^{th} element. For further information on the quantification method, see Malucelli et al. [11].

Results and discussion

We assessed the composition and the elemental distribution of light elements in single cells belonging to three different strains, i.e. human umbilical vein endothelial cells (HUVEC), human osteoblast-like SaOS2, and colon carcinoma LoVo cells. These strains were opportunely treated (see Method section) to induce a possible variation in the total Mg content. We applied a multimodal/multiscale approach, which merges complementary techniques as AFM, synchrotron XRFM, and scanning transmission X-ray microscopy (STXM) [11, 12]. This approach allows us to obtain nanoscale maps of morphological variables (mass, volume and density) and compositional quantities (mass fraction and

concentration). We quantified and mapped the fundamental life elements, C, N, and O, and the light metal Mg (Fig. 1) in whole dehydrated single cells. All the variables derived by single cell analysis for the three different cellular strains are reported in ESM Tables S1, S2, and S3. In order to check the reproducibility and reliability of the single cells analysis, we performed the statistical analysis between control and treated cells of the same cell lines. The comparison did not show any statistical differences, either in morphological variables or in the concentration of fundamental elements (C, N, O) in all three cell types. The average of the total mass fraction (W_{tot}) for each group of cells ranged between 80% and 91% in all the single cells analyzed. The missing mass fraction, accounting for about 7%–10%, is predominantly given by the elements P and H, which were not taken into consideration by our analysis [30]. Regarding the different preparation procedures, adopted in LoVo cell, it can be noted that there are no significant differences in the mean values of total element mass fraction and concentration between chemically fixed and freeze-dried cells as already reported in [11]. This result demonstrates the reliability of the quantitative method adopted, which includes the correction for the self-absorption effect, mandatory for light element such as C, N, and O, whereas for Mg this effect is weaker [32]. The self-absorption correction requires the knowledge of both volume and density of the sample [25]. The quantification of the volume (derived by AFM) is fundamental to calculate the elemental concentration as well.

Focusing the attention on the Mg concentration, Fig. 2 shows a statistically significant decrease of the element in starved SaOS2 cells maintained in Mg free medium versus controls (33 ± 8 mM in $\text{SaOS2}^{-\text{Mg}}$; 92 ± 7 mM in $\text{SaOS2}^{+\text{Mg}}$; $p < 0.001$). It is worthy to note the small variability (small SD) of Mg concentration in SaOS2 experiments both in $\text{SaOS2}^{-\text{Mg}}$ and in $\text{SaOS2}^{+\text{Mg}}$ with respect to LoVo and HUVEC. This result can be ascribed to the deprivation of Mg, which is known to cause synchronization in G0/G1 phase (see ESM Fig. S1) leading to a more homogenous cell population. It could also be due to the fact that Mg deprivation prevents Mg fluctuations during the different phases of the cell cycle [33]. We also found a slightly higher Mg concentration in LoVo-R than in LoVo-S, on the borderline of statistical significance ($p < 0.05$). This difference is entirely due to the extremely high values found in two LoVo-R cells than in the other sister cells. In fact, performing the statistical analysis without taking into account these two LoVo-R does not highlight any difference in the Mg content in the two populations. Nevertheless, these two cells have all the other constitutive elements quantified (C, O, N) as well as all the morphological quantities matching perfectly those of the other LoVo-R sister cells. Therefore, this result would suggest that the higher Mg concentration found in LoVo-R, which has already been reported in other studies [18, 29], could be due to the

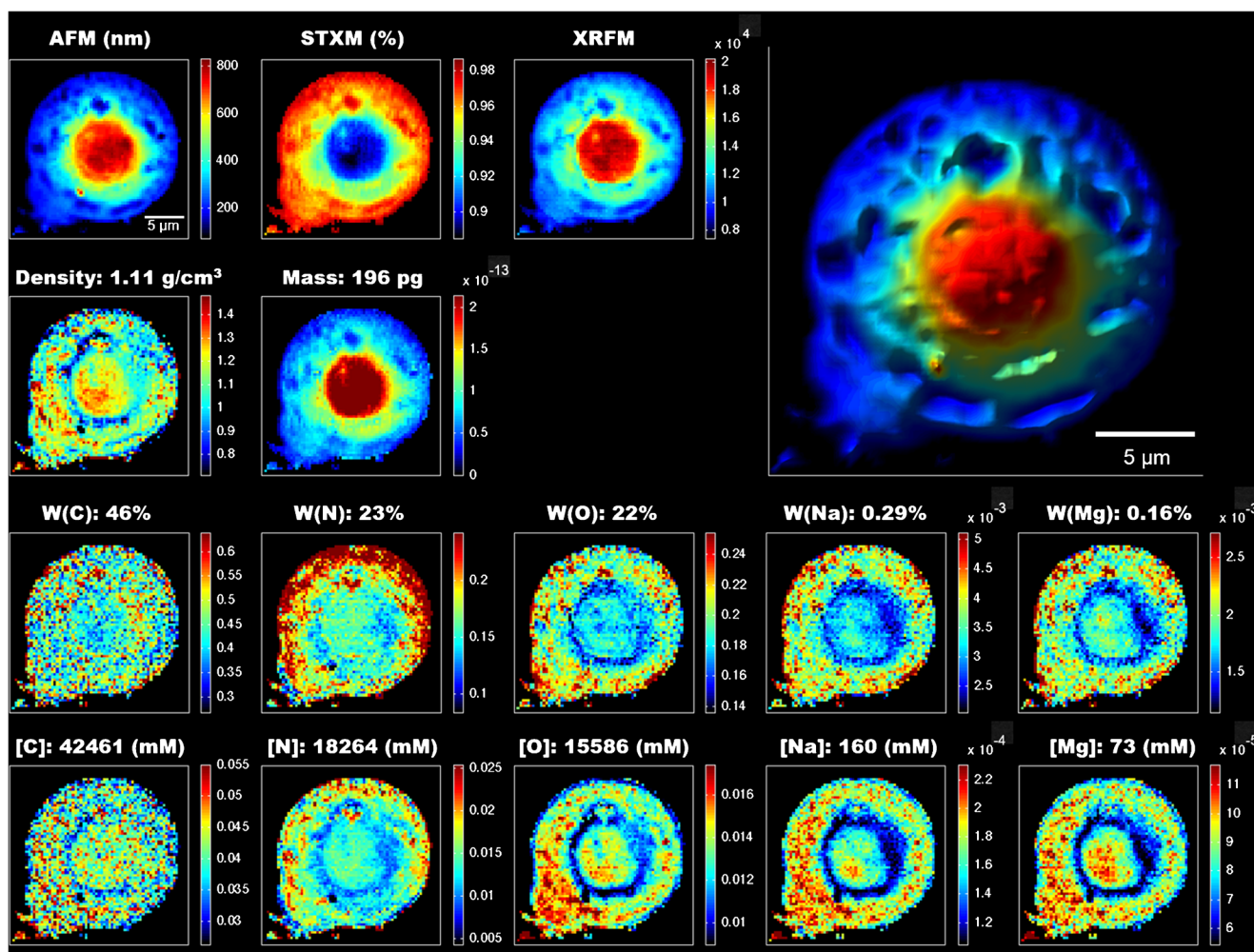


Fig. 1 (Top row, from the left) morphology, X-ray transmission, and X-ray fluorescence images of a colon adenocarcinoma cell LoVo, acquired by atomic force microscopy (AFM), scanning transmission X-ray microscopy (STXM), and X-ray fluorescence microscopy (XRFM), respectively. The XRFM image reports the sum of all the channels of

the spectrum. In the top right panel a 3D rendering of AFM is shown. A nanoscale map of the spatial distribution of the cell density and mass is then calculated from AFM and STXM (second row). The third and fourth rows show elemental nanoscale maps of mass fraction and molar concentration of C, N, O, Na, and Mg

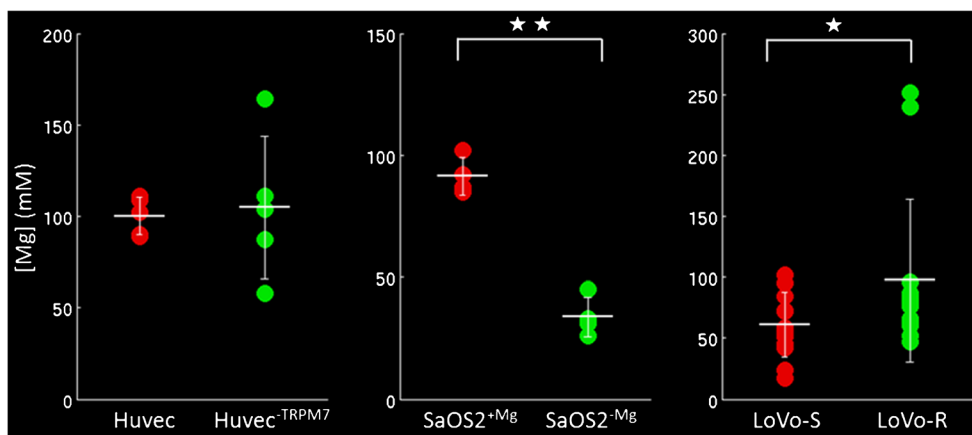


Fig. 2 The scatter plot of the total intracellular Mg concentration assessed by single cells analysis (XRFM and AFM) for the three different cellular strains (HUVEC, SaOS2, and LoVo) both in control (red dots) and in treated cells (green dots). Horizontal white lines

indicate the mean Mg concentrations, and whiskers indicate the standard deviation. Each control strain is compared with the respective treated using a one-tail *t*-test. The results are reported as critical significance levels: <0.001 (★) and 0.05 (★★)

heterogeneity in the Mg intracellular content of the population of this cell strain. A higher Mg intracellular content in drug-resistant cell populations has also been found in cisplatin-resistant human ovarian cancer cells [34]. Therefore, it seems that a higher intracellular Mg concentration represents a feature linked to the cancer drug-resistance. However, if the higher amount of Mg with LoVo-R rather than LoVo-S is a reproducible feature, in our experience the amount of this over-quantity is quite variable (compare data of reference [29] with this study). We hypothesize that this trait could be a consequence of the heterogeneity in Mg intracellular content of this cell type.

Single cell analysis performed on HUVEC cells did not show any difference in the Mg content in HUVEC^{-TRPM7} with respect to their controls, suggesting that other transporters operate Mg entry in this cell line. Some degree of heterogeneity in the intracellular Mg concentration is also visible in HUVEC^{-TRPM7} cells, although not so dramatic as that found in LoVo-R.

The aim of this study is to evaluate how the intrinsic heterogeneity of a cell population affects the elemental composition. Therefore, we compared the Mg content measured in single cells with that of a population of cells. While being mindful of the inherent limitations of such an approach, as single cell analysis by definition is not representative of the cell population, we deliberately pursued this task to understand how the analysis of the content of an essential element such as Mg measured in single cell can be comparable to that measured in the whole population. For this purpose we quantified the total amount of intracellular Mg in a large population of the same cell types exploiting the specific fluorescent chemosensor (DCHQ5) developed in our laboratory [18]. The peculiarity of DCHQ5 is the capability to analyze the total cellular amount of Mg, differently from the Mg commercial probes, which quantify the ionic fraction only [35]. To obtain the Mg molar concentration of the investigated cell population, we normalized the amount of Mg assessed by fluorimetric assay to the cell volume of the strain population assessed by the Z1 Beckman Coulter Counter. The volume has been calculated for the three cell lines both in controls and in conditioned samples. HUVEC^{-TRPM7} cells did not show any difference in the Mg content with respect to controls (see ESM Table S4), whereas the content of Mg was different with respect to controls both in LoVo, ($p < 0.05$) (see ESM Table S5) and in SaOS2 cells, ($p < 0.01$) (see ESM Table S6). The concentration of total Mg obtained by DCHQ5 measurements reflects the results obtained by single cell analysis. This result discloses the ability of the single cell approach to reveal the same differences found in a large population of cells (Table 1). In particular, DCHQ5 chemosensor showed a high sensitivity in detecting a slight statistically significant difference between LoVo-S (18.4 ± 1.4 mM) and LoVo-R (20.4 ± 1.6 mM), denoting a small coefficient of variation (Table 1).

These results can lead to a consideration deriving from the descriptive statistic and the concepts of large population and small population. The total content of intracellular Mg using DCHQ5 chemosensor is performed in a population of cells and the descriptive statistics is obtained from different measurements achieved in the same conditions. As a consequence, the biological variability of the cells population is not taken into account or is mitigated by the large amount of cells. Therefore, the descriptive statistic for each cell line describes the reproducibility of the experiment and the precision of the techniques applied. In single cell analysis we analyzed a small amount of cells describing a micro population. In this case, the descriptive statistic is not robust and in principle may yield to different results for different micro populations. On the other hand, in single cell analysis the possible influence of the biological variability of the population is relevant, leading to higher standard deviations.

We purposely applied the parametric statistics on single cell data, being aware that it is appropriate for large populations and not for small populations. Indeed, a cell population consists of individual cells and complex mathematical models have been proposed to solve this puzzling issue such as the “cell population balance model” that takes into account the heterogeneous and distributed nature of cells by recognizing that a cell population consists of individual cells [36]. Despite all these considerations, we found very coherent results comparing single cells and large population analysis.

Single cell analysis revealed a much higher amount of intracellular Mg (about four times) in two cells (Fig. 2, LoVo panel), as reported above. Therefore the higher Mg concentration found in the population of LoVo-R analyzed as a whole using chemosensor does not represent a uniform mark characterizing all cells of the population, but rather a consequence of a skewed distribution.

The intracellular concentration of Mg calculated by single cell analysis is higher than Mg content obtained by cell population analysis, although in the same order of magnitude. These results are due to the fixation method; in fact single cell measurements by XRFM requires dehydrated cells, a procedure that intrinsically leads to a reduction of volume about five times [37, 38]. This hampers a direct comparison of intracellular Mg concentration assessed in single cells and in cell population, since a reduction of volume implicates an increase in concentration of the analyte. Based on these considerations, the values of intracellular Mg concentration obtained in single cell measurements are even more alike to those obtained in large population assays.

This study fulfilled the goal of comparing the concentrations of a light essential chemical element quantified in single cells and in a large population of cells. Recent literature reports some studies that use XRFM and/or inductively coupled plasma mass spectrometry to explore the intracellular content variability of both endogenous and exogenous heavy elements

Table 1 shows the total Mg evaluated by the cell population analysis using the DCHQ5 chemosensor and by the single cell analysis using XRFM. All the data (mean \pm standard deviation) are reported both in controls and in treated cells of the three strains (HUVEC, SaOS2, and LoVo). Each control strain is compared with the respective treated using a one-tail *t*-test. The results are reported as critical significance levels: < 0.01 (★★) and 0.05 (★)

	HUVEC	HUVEC ^{-TRPM7}	SaOS2 ^{+Mg}	SaOS2 ^{-Mg}	LoVo-S	LoVo-R
DCHQ5 (mM)	22.5 \pm 1.1	23.1 \pm 1.6	13.8 \pm 0.9	8.1 \pm 0.7 ★★	18.4 \pm 1.3	20.4 \pm 1.5★
XRFM (mM)	100 \pm 10	105 \pm 39	92 \pm 7	33 \pm 8 ★★	61 \pm 27	97 \pm 27 ★

in a population of single cells [39–42]. Among these, one study compares the intracellular concentration of TiO₂ nanoparticles assessed in single cells and in a cell population [39], finding that the nanoparticles concentration was of one to two orders of magnitude greater in single cells compared with the average value obtained in cell population. However, our study shows that the assessment of intracellular Mg in single cells gives consistent and comparable results to those obtained in large population assays, hence opening new perspectives in the applications of XRFM in single cells analysis.

Imaging analysis

DCHQ5 dye, in addition to quantitative assays, allows visualizing the intracellular Mg distribution in single living cells using confocal fluorescence microscopy (see ESM Fig. S2). However, DCHQ5 does not permeate both the nuclear and mitochondria membrane [43, 44], hence the visualization of intracellular Mg is restricted to the cytosol and plasma membrane. DCHQ5 as well as the other chemosensors do not allow the concentration assessment by imaging. Rather, the single cell analysis by XRFM allows mapping the intracellular Mg concentration and other light elements in whole cells at much higher spatial resolution, starting from 500 nm for light elements, down to 50 nm for heavier elements such as transition metals [12, 16, 24]. We exploited this feature to perform a detailed intensity correlation analysis (ICA) [45, 46] on the two LoVo-R cells with the highest Mg content. We aimed to explore if the high Mg concentration resulted in a different subcellular distribution. To this purpose, we correlated the Mg distribution to the constitutive element oxygen, the concentration and distribution of which are similar in all analyzed cells. The following description of ICA is based on McRae et al. [46]: “ICA describes the extent of synchronous variations between two species X and Y by the product $(X_i - \bar{x})(Y_i - \bar{y})$, where \bar{x} and \bar{y} correspond to the mean intensities of X_i and Y_i of the pixels i within a region of interest [45]”. Positive product values indicate a dependent intensity variation and thus co-localization, whereas negative values occur in the case of spatially segregated species. Furthermore, the intensity correlation

quotient (ICQ), defined as the ratio between pixels with a positive product and the total number of pixels subtracted by 0.5, is a direct measure of co-localization. Therefore, values range between -0.5 and $+0.5$, where negative numbers indicate segregation, near zero values a random distribution, and positive values a dependent relationship”.

The results of ICA performed on the two chemically fixed LoVo-R cells with the highest intracellular Mg concentration (H-MagIC) were compared with ICA performed on other two chemically fixed LoVo-R cells (Fig. 3 first row) with average Mg concentration. ICA yielded positive ICQ values (0.37, 0.26, 0.34, and 0.33) indicating a synchronous variation of the respective elemental concentration. In particular, the two H-MagIC LoVo-R showed a similar pattern of ICA values distribution depicting a strong co-localization (high ICA value) of O and Mg concentration in the peripheral area. On the other hand, the LoVo-R cells showed a different pattern (Fig. 3 second row) with a more homogeneous co-localization (high ICA value in yellow/orange) of O and Mg concentration. The synchronously correlated pixels, with positive ICA and Mg concentration over the mean value, highlighted in yellow in the scatter plot (Fig. 3 third row), covered precisely the nucleus area in the LoVo-R, whereas in the H-MagIC LoVo-R cells the synchronous correlation was more evident in the perinuclear area (Fig. 3 fourth row). For all ICAs, the number of segregated pixels (green and red) with a negative ICA product is low and shows a mostly random distribution. In conclusion, this analysis reveals that the H-MagIC LoVo-R cells display a different Mg subcellular compartmentalization of Mg and O compared with the other LoVo-R cells, which is a high accumulation of both Mg and O in the peripheral area corroborating the preliminary results reported in Malucelli et al. [11].

Moreover, we analyzed the correlation between the thickness and the mass, which are experimental quantities coming directly from AFM and STXM measurements, respectively (see ESM Fig. S3 panels A and B), and hence not affected by any propagation errors due to post-processing analysis. The mass and the volume were linearly correlated, with near-unity, Pearson coefficients of 0.98 (see ESM Fig. S3 panel C). The ICA showed a black and circular area within the cell depicting a region where the mass and the volume were simultaneously close to their mean values. Moreover,

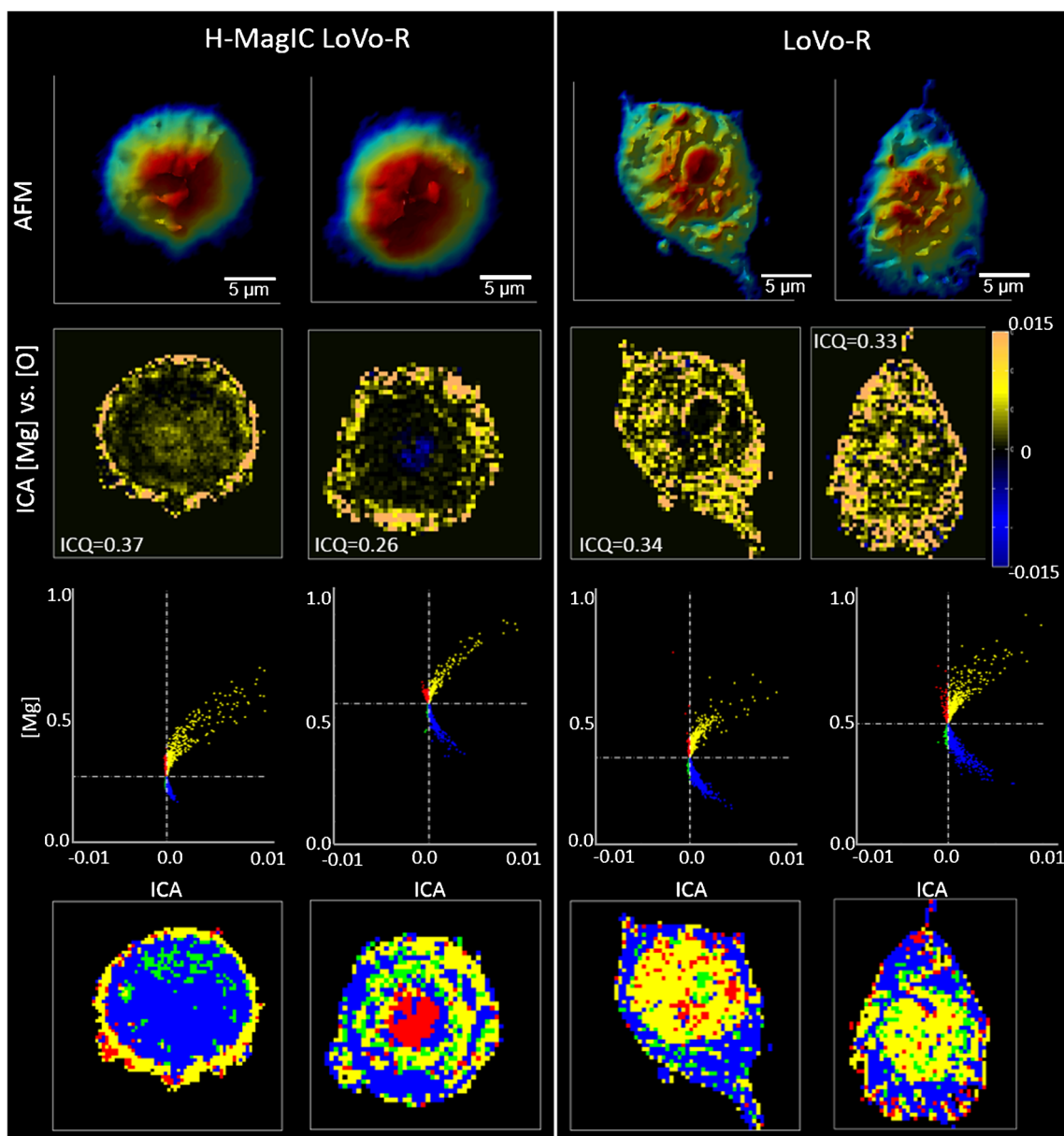


Fig. 3 The ICA analysis of the two highest intracellular Mg concentration (H-MagIC) LoVo-R cells compared with two LoVo-R cells. The first row shows 3D reconstruction of the cells using the thickness maps derived by the AFM. The second row depicts the map of the intracellular correlation of Mg and O concentrations assessed by intensity correlation ratio (ICA). Positive values (yellow scale) indicate a dependent intensity variation of Mg and O, thus co-localization, whereas negative values (blue scale) occur in the case of spatially segregated species. The positive ICQ values determine the rate of dependent

the ICA analysis did not show any blue pixel; thus volume and mass were simultaneously over and under their mean values (ICQ = 0.47) (see ESM Fig. S3 panel D). This pattern was common to all the analyzed cells. The scatter plot of the ICA values highlights an equal trend of the two variables; in the nuclear area they were higher than their mean values decreasing towards the mean values (black perinuclear circle); on the other hand in

relationship. The third row illustrates the scatter plot of intracellular ICA values versus the Mg concentration; vertical dashed line indicates the value 0 of ICA and the horizontal dashed line indicates the mean intracellular concentration of Mg. The yellow dot shows positive values of ICA and values of Mg concentration over its intracellular mean (correlated). Blue dots represent positive values of ICA, Mg, and O concentration below the mean. The fourth row shows the intracellular localization of the scatter plots of the third row

the peripheral area they were both less than the mean values as shown in ESM Fig. S3 panels E and F.

Conclusion

Single cell and cell population analyses of the intracellular total magnesium concentration display the same statistically

significant results between control and treated cells of the same strains. The inherent limitation of single cell analysis approach has been shown to be manageable as far as the intracellular content of this essential element. However, some caution must be taken to generalize this result. The single cell analysis approach here presented also provides information about the intracellular compartmentalization of elemental concentration. In fact, the information provided by single cell and large population analyses are different but complementary, and it is advisable to exploit the opportunity to merge, when possible, the two approaches.

Compliance with ethical standards

Conflict of interest The authors declare that there are no conflicts of interest.

References

- Stockholm D, Benchaouir R, Picot J, Rameau P, Neildez TMA, Landini G, Laplace-Builh c C, Paldi A (2007) The origin of phenotypic heterogeneity in a clonal cell population in vitro. *PLoS ONE*. doi: <https://doi.org/10.1371/journal.pone.0000394>
- Vallejos CA, Marioni JC, Richardson S. BASiCS: Bayesian analysis of single-cell sequencing data. *PLoS Comput Biol*. 2015;11:e1004333.
- Amantonico A, Urban PL, Zenobi R. Analytical techniques for single-cell metabolomics: state of the art and trends. *Anal Bioanal Chem*. 2010;398:2493–504.
- Lin Y, Trouillon R, Safina G, Ewing AG. Chemical analysis of single cells. *Anal Chem*. 2011;83:4369–92.
- Li L, Fan Y, Li Q, Sheng R, Si H, Fang J, et al. Simultaneous single-cell analysis of Na⁺, K⁺, Ca²⁺, and Mg²⁺ in neuron-like PC-12 cells in a microfluidic system. *Anal Chem*. 2017;89:4559–65.
- Templer RH, Ces O. New frontiers in single-cell analysis. *J R Soc Interface*. 2008;5:S111–2.
- Birtwistle MR, Rauch J, Kiyatkin A, Aksamitiene E, Dobrzyński M, Hoek JB, et al. Emergence of bimodal cell population responses from the interplay between analog single-cell signaling and protein expression noise. *BMC Syst Biol*. 2012;6:109.
- Yin H, Marshall D. Microfluidics for single cell analysis. *Curr Opin Biotechnol*. 2012;23:110–9.
- Mack E, Neubauer A, Brendel C. Comparison of RNA yield from small cell populations sorted by flow cytometry applying different isolation procedures. *Cytometry A*. 2007;71A:404–9.
- Wang D, Bodovitz S. Single cell analysis: the new frontier in “omics.”. *Trends Biotechnol*. 2010;28:281–90.
- Malucelli E, Iotti S, Gianoncelli A, Fratini M, Merolle L, Notargiacomo A, et al. Quantitative chemical imaging of the intracellular spatial distribution of fundamental elements and light metals in single cells. *Anal Chem*. 2014;86:5108–15.
- Lagomarsino S, Iotti S, Farruggia G, Cedola A, Trapani V, Fratini M, et al. Intracellular concentration map of magnesium in whole cells by combined use of X-ray fluorescence microscopy and atomic force microscopy. *Spectrochim Acta B At Spectrosc*. 2011;66:834–40.
- Kaulich B, Gianoncelli A, Beran A, Eichert D, Kreft I, Pongrac P, et al. Low-energy X-ray fluorescence microscopy opening new opportunities for bio-related research. *J R Soc Interface*. 2009;6:S641–7.
- Paunesku T, Vogt S, Lai B, Maser J, Stojicevic N, Thum KT, et al. Intracellular distribution of TiO₂-DNA oligonucleotide nanoconjugates directed to nucleolus and mitochondria indicates sequence specificity. *Nano Lett*. 2007;7:596–601.
- Carmona A, Dev s G, Ortega R. Quantitative micro-analysis of metal ions in subcellular compartments of cultured dopaminergic cells by combination of three ion beam techniques. *Anal Bioanal Chem*. 2008;390:1585–94.
- Kosior E, Bohic S, Suhonen H, Ortega R, Dev s G, Carmona A, et al. Combined use of hard X-ray phase contrast imaging and X-ray fluorescence microscopy for sub-cellular metal quantification. *J Struct Biol*. 2012;177:239–47.
- Marmorato P, Ceccone G, Gianoncelli A, Pascolo L, Ponti J, Rossi F, et al. Cellular distribution and degradation of cobalt ferrite nanoparticles in Balb/3T3 mouse fibroblasts. *Toxicol Lett*. 2011;207:128–36.
- Sargenti A, Farruggia G, Zaccheroni N, Marraccini C, Sgarzi M, Cappadone C, et al. Synthesis of a highly Mg²⁺-selective fluorescent probe and its application to quantifying and imaging total intracellular magnesium. *Nat Protoc*. 2017;12:461–71.
- Sargenti A, Farruggia G, Malucelli E, Cappadone C, Merolle L, Marraccini C, et al. A novel fluorescent chemosensor allows the assessment of intracellular total magnesium in small samples. *Analyst*. 2014;139:1201–7.
- Murphy E. Mysteries of Magnesium Homeostasis. *Circ Res*. 2000;86:245–8. <https://doi.org/10.1161/01.RES.86.3.245>.
- Carmona A, Cloetens P, Dev s G, Bohic S, Ortega R. Nano-imaging of trace metals by synchrotron X-ray fluorescence into dopaminergic single cells and neurite-like processes. *J Anal At Spectrom*. 2008;23:1083–8.
- Ortega R, Dev s G, Carmona A. Bio-metals imaging and speciation in cells using proton and synchrotron radiation X-ray microspectroscopy. *J R Soc Interface*. 2009;6:S649–58. <https://doi.org/10.1098/rsif.2009.0166.focus>.
- Kopittke PM, Moore KL, Lombi E, Gianoncelli A, Ferguson BJ, Blamey FPC, et al. Identification of the primary lesion of toxic aluminum in plant roots1. *Plant Physiol*. 2015;167:1402–11.
- Vogt S, Lai B, Finney L, Palmer B, Wu L, Harris H, et al. Imaging trace elements in cells with X-ray fluorescence microscopy. *Microsc Microanal*. 2007;13:40–1.
- Malucelli E, Fratini M, Notargiacomo A, Gianoncelli A, Merolle L, Sargenti A, et al. Where is it and how much? Mapping and quantifying elements in single cells. *Analyst*. 2016;141:5221–35.
- Baldoli E, Castiglioni S, Maier JAM (2013) Regulation and function of TRPM7 in human endothelial cells: TRPM7 as a potential novel regulator of endothelial function. *PLoS ONE*. doi: <https://doi.org/10.1371/journal.pone.0059891>
- Castiglioni S, Cazzaniga A, Trapani V, Cappadone C, Farruggia G, Merolle L, et al. Magnesium homeostasis in colon carcinoma LoVo cells sensitive or resistant to doxorubicin. *Sci Rep*. 2015;5:16538.
- Gianoncelli A, Kourousias G, Merolle L, Altissimo M, Bianco A. Current status of the TwinMic beamline at Elettra: a soft X-ray transmission and emission microscopy station. *J Synchrotron Radiat*. 2016;23:1526–37.
- Janssens KHA, Adams FCV, Rindby A. Microscopic X-ray fluorescence analysis. New York: John Wiley and Sons Ltd.; 2000.
- von Stockar U, Liu J-S. Does microbial life always feed on negative entropy? Thermodynamic analysis of microbial growth. *Biochim Biophys Acta BBA – Bioenerg*. 1999;1412:191–211.
- Sol  VA, Papillon E, Cotte M, Walter P, Susini J. A multiplatform code for the analysis of energy-dispersive X-ray fluorescence spectra. *Spectrochim Acta B At Spectrosc*. 2007;62:63–8.
- Malucelli E, Iotti S, Fratini M, Marraccini C, Notargiacomo A, Gianoncelli A, et al. X-ray fluorescence microscopy of light elements in cells: self-absorption correction by integration of

- compositional and morphological measurements. *J Phys Conf Ser.* 2013;463:012022.
33. Wolf FI, Trapani V, Simonacci M, Boninsegna A, Mazur A, Maier JAM. Magnesium deficiency affects mammary epithelial cell proliferation: involvement of oxidative stress. *Nutr Cancer.* 2009;61:131–6.
 34. Marverti G, Ligabue A, Montanari M, Guerrieri D, Cusumano M, Pietro MLD, et al. Characterization of the cell growth inhibitory effects of a novel DNA-intercalating bipyridyl-thiourea-Pt(II) complex in cisplatin-sensitive and -resistant human ovarian cancer cells. *Investig New Drugs.* 2011;29:73–86.
 35. Farruggia G, Iotti S, Prodi L, Zaccheroni N, Montalti M, Savage PB, et al. A simple spectrofluorometric assay to measure total intracellular magnesium by a hydroxyquinoline derivative. *J Fluoresc.* 2008;19:11.
 36. Mantzaris NV, Daoutidis P, Srien F. Numerical solution of multi-variable cell population balance models: I. Finite difference methods. *Comput Chem Eng.* 2001;25:1411–40.
 37. Gusnard D, Kirschner RH. Cell and organelle shrinkage during preparation for scanning electron microscopy: effects of fixation, dehydration, and critical point drying. *J Microsc.* 1977;110:51–7.
 38. Bacallao R, Stelzer EHK. Chapter 20. Preservation of biological specimens for observation in a confocal fluorescence microscope and operational principles of confocal fluorescence microscopy. *Methods Cell Biol.* 1989;31:437–52.
 39. Rashkow JT, Patel SC, Tappero R, Sitharaman B. Quantification of single-cell nanoparticle concentrations and the distribution of these concentrations in cell population. *J R Soc Interface.* 2014;11:20131152.
 40. James SA, Feltis BN, de Jonge MD, Sridhar M, Kimpton JA, Altissimo M, et al. Quantification of ZnO nanoparticle uptake, distribution, and dissolution within individual human macrophages. *ACS Nano.* 2013;7:10621–35.
 41. Turnbull T, Douglass M, Paterson D, Bezak E, Thierry B, Kempson I. Relating intercellular variability in nanoparticle uptake with biological consequence: a quantitative X-ray fluorescence study for radiosensitization of cells. *Anal Chem.* 2015;87:10693–7.
 42. Wang H, Wang B, Wang M, Zheng L, Chen H, Chai Z, et al. Time-resolved ICP-MS analysis of mineral element contents and distribution patterns in single cells. *Analyst.* 2014;140:523–31.
 43. Farruggia G, Iotti S, Prodi L, Montalti M, Zaccheroni N, Savage PB, et al. 8-Hydroxyquinoline derivatives as fluorescent sensors for magnesium in living cells. *J Am Chem Soc.* 2006;128:344–50.
 44. Marraccini C, Farruggia G, Lombardo M, Prodi L, Sgarzi M, Trapani V, et al. Diaza-18-crown-6 hydroxyquinoline derivatives as flexible tools for the assessment and imaging of total intracellular magnesium. *Chem Sci.* 2012;3:727–34.
 45. Li Q, Lau A, Morris TJ, Guo L, Fordyce CB, Stanley EF. A Syntaxin 1, G α , and N-type calcium channel complex at a pre-synaptic nerve terminal: Analysis by Quantitative Immunocolocalization. *J Neurosci.* 2004;24:4070–81.
 46. McRae R, Lai BJ, Fahrni C. Subcellular redistribution and mitotic inheritance of transition metals in proliferating mouse fibroblast cells. *Metallomics.* 2013;5:52–61.



Emil Malucelli is Assistant Professor at the University of Bologna. He contributed to the development of *in vivo* magnetic resonance spectroscopy and imaging for the study of neurological disease. Now he is devoted to cellular imaging using X-ray synchrotron-based techniques that are useful for the elemental, morphological and functional characterization of single cells.



Alessandra Procopio is a PhD student in biotechnological and pharmaceutical sciences at the University of Bologna. Her research activity is focused on cellular imaging using X-ray synchrotron-based techniques such as X-ray fluorescence microscopy, phase-contrast imaging (2D) and nanotomography (3D).



Michela Fratini obtained her Master's degree in Physics (2004), as well as her Specialization in Medical Physics (2008), from Sapienza University of Rome. In 2016, she earned a PhD degree in Physics at the University of Roma-Tre. Most of her experimental work (chiefly performed at Elettra, ESRF, APS, PSI-SLS facilities) is based on X-ray diffraction, fluorescence and phase contrast tomography.



Alessandra Gianoncelli is head of the TwinMic X-ray Microscopy beamline at Elettra Sincrotrone Trieste, Italy. She has been working for several years on the soft X-ray microscopy and X-ray fluorescence fields, complementing them with diverse analytical techniques (AFM, FTIR, SEM...) for biological systems' and materials' characterization and analysis. She is co-author of more than 110 articles in reviewed journals and she holds an international patent concerning an innovative X-ray diffraction (XRD) system.

international patent concerning an innovative X-ray diffraction (XRD) system.



Azzurra Sargenti in 2012 received a Master's degree in Medical Biotechnology. In 2016 she received a PhD degree in Biochemical and Biotechnological Sciences from the Department of Pharmacy and Biotechnology of Bologna University. The main topics of her research focus on the biological application of new biosensors for the assessment and imaging of total intracellular magnesium.



Andrea Notargiacomo is a researcher at the Institute for Photonics and Nanotechnology (National Research Council of Italy – CNR). His main research interests focus on mesoscopic physics in Si/SiGe, scanning probe imaging and lithography, fabrication of ZnO based devices.



Sara Castiglioni is Assistant Professor of General Pathology at the Department of Biomedical and Clinical Sciences L. Sacco of University of Milan, Italy. With a degree in Biological Science (2003) and PhD in Molecular Medicine (2008), she has a strong expertise in cellular and molecular biology. Her areas of research include endothelium, bone mesenchymal stem cells, magnesium homeostasis, signal transduction and cell microgravity. She is co-author of more than 30 original papers published in peer-reviewed journals.

tion and cell microgravity. She is co-author of more than 30 original papers published in peer-reviewed journals.



Lucia Merolle received a Master's degree in Pharmaceutical Chemistry and Technology (2011) as well as her PhD degree in Biochemical and Biotechnological Sciences (2015) from Bologna University. The same year she won a post-doc position at the Elettra Synchrotron, Trieste, Italy. Now she is pursuing her research activity, mainly focused on transfusion medicine and cancer therapy, at the AUSL-IRCCS Reggio Emilia, Italy.



Concettina Cappadone is Assistant Professor at the Department of Pharmacy and Biotechnology of the University of Bologna. The main topics of her research concern the control mechanisms of cell proliferation and cell death in pathophysiological conditions, with focus on the role of magnesium in these processes. At present, her interest is in exploring different technical approaches to obtain cell elemental maps.



Giovanna Farruggia is Assistant Professor at the Department of Pharmacy and Biotechnology of the University of Bologna. Her research mainly concerns the photochemical properties of new biosensors for intracellular cations, by integrating spectroscopic, microscopic and cytofluorimetric approaches. Her main interest is the application of such indicators to the study of magnesium cellular and tissutal homeostasis in physiological and pathological conditions.



Jeanette A. Maier is full professor and head of the General Pathology Lab at the University of Milan. She was trained in the USA on the pathophysiology of the endothelium, with a focus on aging and senescence. For the last 15 years she investigated the response of vascular cells to magnesium and to the silencing of its transporters. Lately, her attention has been devoted also to the role of magnesium in bone homeostasis.



Marco Lombardo is Associate Professor of Organic Chemistry at the University of Bologna. His main research interests are the development of new methodologies in synthetic organic chemistry and the synthesis of new molecules for applications in analytical and in medicinal chemistry.



Stefano Iotti is Professor of Biochemistry at the Bologna University. He contributed to the development of in vivo MR spectroscopy in basic research and in diagnostic applications and of a novel approach to treat the thermodynamics of complex systems. His scientific activity ranged from organic and physical chemistry to biochemical thermodynamics. Recently, his research activity is devoted to the study of magnesium homeostasis.



Stefano Lagomarsino has been Researcher and Research Director in Physics of X-rays at National Research Council (CNR) of Italy for more than 40 years. He is now retired but he continues to collaborate as Associated Researcher at the Institute of Nanotechnology of CNR.